PHOTOPHYSICAL STUDIES OF OPTICALLY ACTIVE POLY(PYRIDYL)-RUTHENIUM(II) CHELATES ION-EXCHANGED ON Na-HECTORITE CLAY

VISHWAS JOSHI, DILIP KOTKAR and PUSHPITO K. GHOSH
Alchemie Research Centre, P.O. Box 155, Thane-Belapur Road, Thane 400 601, India.

ABSTRACT

UV-vis absorption and emission spectral studies of enantiomeric and racemic RuL_3^{2+}-hectorite (L = 1,10-phenanthroline; 2,2'-bipyridine) adsorbates are reported. Differences in the spectral behaviour of the enantiomeric and racemic forms are rationalized as arising from interaction(s) between optical antipodes, either in the final state or during the process of sorption. Results of luminescence quenching studies with methyl viologen (MV^{2+}) and (−)-$Co(edta)^-$ are also discussed.

INTRODUCTION

THERE is considerable interest in the study of binding modes of chiral compounds in smectite clays since such clay types may have played an important role in the natural chiral selection process during prebiotic evolution[1,2]. Moreover, a detailed understanding of clay-molecule interactions may permit development of clay-based chromatographic columns for optical resolution and solid-supported stereoselective synthesis of organic molecules[1,3–5].

The study of optically active poly(pyridyl) metal complex-clay intercalates has been of some interest, in this regard. Such complexes are useful probes since they are amenable to routine spectroscopic investigation and can be readily converted into the pure enantiomeric forms[6]. Yamagishi and coworkers have suggested that such complexes exist as racemic pairs within the clay matrix, and have illustrated the potential applications of chirally modified clays[3,5,7,8]. More recently, this laboratory has provided direct spectroscopic evidence for interactions between optical antipodes, even when these complex ions are seemingly lightly packed in the clay interlayer[9,10]. As part of our ongoing research in this area, we now wish to highlight the luminescence profiles of $Ru(bpy)_3^{2+}$ and $Ru(phen)_3^{2+}$ (bpy = 2,2'-bipyridine; phen = 1,10-phenanthroline) adsorbed on Na-hectorite clay. In addition, Stern-Volmer plots for the quenching of the adsorbed complexes by methyl violgen (MV^{2+}) and (−)-$Co(edta)^-$ are also reported.

EXPERIMENTAL

Hectorite clay (SHCa-1) and methyl viologen dichloride ($MVCl_2$) were obtained from the Clay Minerals Repository, University of Missouri, and Aldrich Chemical Company, respectively. The clay samples were further treated[11] to obtain aqueous dispersions of Na-hectorite. $Ru(bpy)_3Cl_2$, $Ru(phen)_3Cl_2$ and K[Co(edta)] were synthesized according to literature procedures[12,13]. (−)-$Co(edta)^-$ was obtained through resolution of the racemate with d-$[Co(en)_2(No_2)]NO_3$[14], while the Ru(II) complexes were resolved with potassium antimonyl tartrate[15]. However, in a slight modification of the original procedure, the partially resolved $Ru(bpy)_3^{2+}$ complexes were converted to the bromide salts, which yielded pure enantiomers upon recrystallization from hot water (4 times). Finally, the Ru(II) complexes were redissolved in water and converted into the perchlorate salts. The purity of the metal chelates was checked by elemental analyses and polarimetry, and found to be satisfactory.

Appropriate concentrations of the metal chelates were prepared in water and these solutions were then added to the aqueous Na-hectorite dispersion (±)-Ru(II) was prepared

by pre-mixing aqueous solutions of the (−)- and (+)-enantiomers. Similarly, quenching studies were carried out on samples prepared by pre-mixing the aqueous solutions of the Ru(II) complex and quencher followed by addition into the clay dispersion. All spectra were recorded on fresh samples and adsorption of Ru(II) and MV^{2+} was checked by high speed (16,000 rpm) centrifugation followed by spectral analysis of the supernatant.

UV-vis spectra were recorded on a spectrophotometer (either on a Pye Unicam Model SP8-100 or Shimadzu Model UV-160), while luminescence studies were carried out on a spectrometer (Perkin Elmer, Model LS-5) interfaced to a data station. Optical rotations were measured on a digital polarimeter (JASCO DIP-140) and an elemental analyser (Carlo Erba, Model 1106) was employed for carbon, hydrogen and nitrogen analysis.

RESULTS AND DISCUSSION

Smectite-type clays, such as Na-hectorite (figure 1), consist of a stack of face-to-face aggregates of clay platelets which are held together by non-covalent forces. Each clay platelet, in turn, is constituted for an octahedral layer sandwiched between tetrahedral silicate sheets. Substitution of a part (ca. 10%) of the Mg^{2+} ions in the octahedral layer with Li^+ results in a charge imbalance in the lattice which is compensated by the incorporation of exchangeable cations, e.g. Na^+, both in the interlamellar space as well as on the exterior surface of the clay. Smectite clays such as Na-hectorite possess high surface area and large cation exchange capacity — typically, the values are 700 m^2/g and 1 mequiv/g, respectively[16] — and readily swell in the presence of water or other polar solvents. Such swelling may eventually lead to delamination of clay platelets and concomitant reduction in the size of the clay particles. Indeed the particle size can be reduced sufficiently this way so as to yield colloidal aqueous dispersions with excellent transparency.

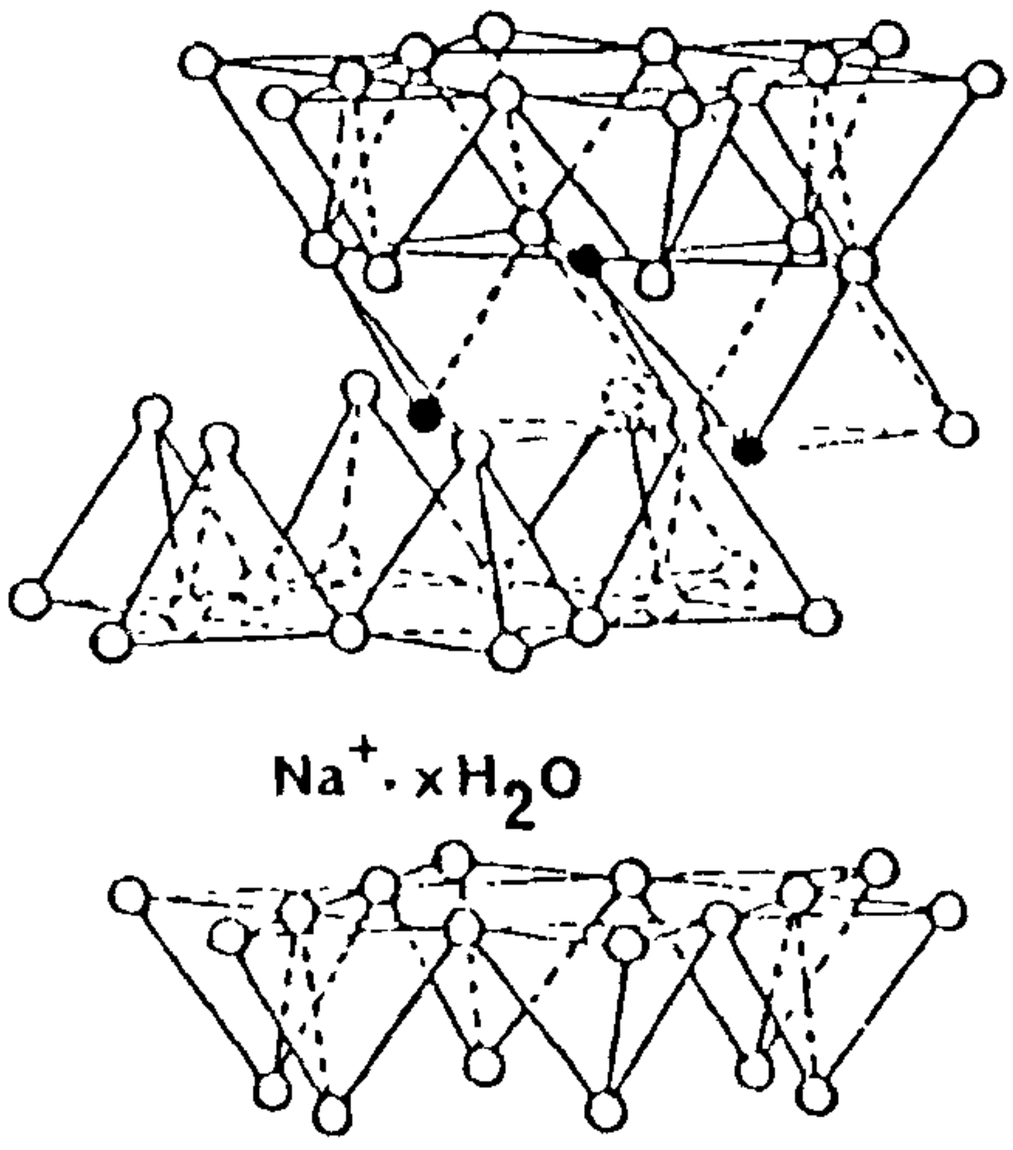

Figure 1. Structure of Na-hectorite clay bearing the unit cell formula $Na_{0.66}[Li_{0.66}Mg_{5.34}](Si_8)$. $O_{20}(OH,F)_4$. (●) = OH/F, (○) = 0. Mg^{2+}/Li^+ occupy the octahedral site while the tetrahedral sites contain Si^{4+}.

The Na^+ ions in Na-hectorite can be readily exchanged with $Ru(bpy)_3^{2+}$ and $Ru(phen)_3^{2+}$ (figure 2). The facile nature of the exchange process is evident from high speed centrifugation of an aqueous dispersion containing 2×10^{-5} M $Ru(bpy)_3^{2+}$ and 1 g/L Na-hectorite, whereupon a colourless supernatant is produced whose spectral analysis suggests complete retention of the Ru(II) complex in clay. The Ru(II) complex has been shown (by X-ray analysis) to intercalate between clay sheets although adsorption of some Ru(II) on the external surface cannot be ruled out[17]. The uv-vis absorption spectrum of (±)-$Ru(bpy)_3^{2+}$-hectorite has been reported by many authors and our own result (figure 3, trace c) is in good agreement with the literature data[11,17a,18]. The spectrum differs substantially from that of the racemate in water (not shown in the figure); e.g. a 17 mm red shift in the metal-to-ligand charge transfer (MLCT) maximum (λ_{max}(MLCT) = 469 nm in Na-hectorite vs. 452 nm in water), with an accompanying increase (ca. 30%) in molar absorptivity. These spectral changes were earlier attributed to clay-molecule interactions[17a]. However, previous results[11] had indicated a non-statistical distribution of the

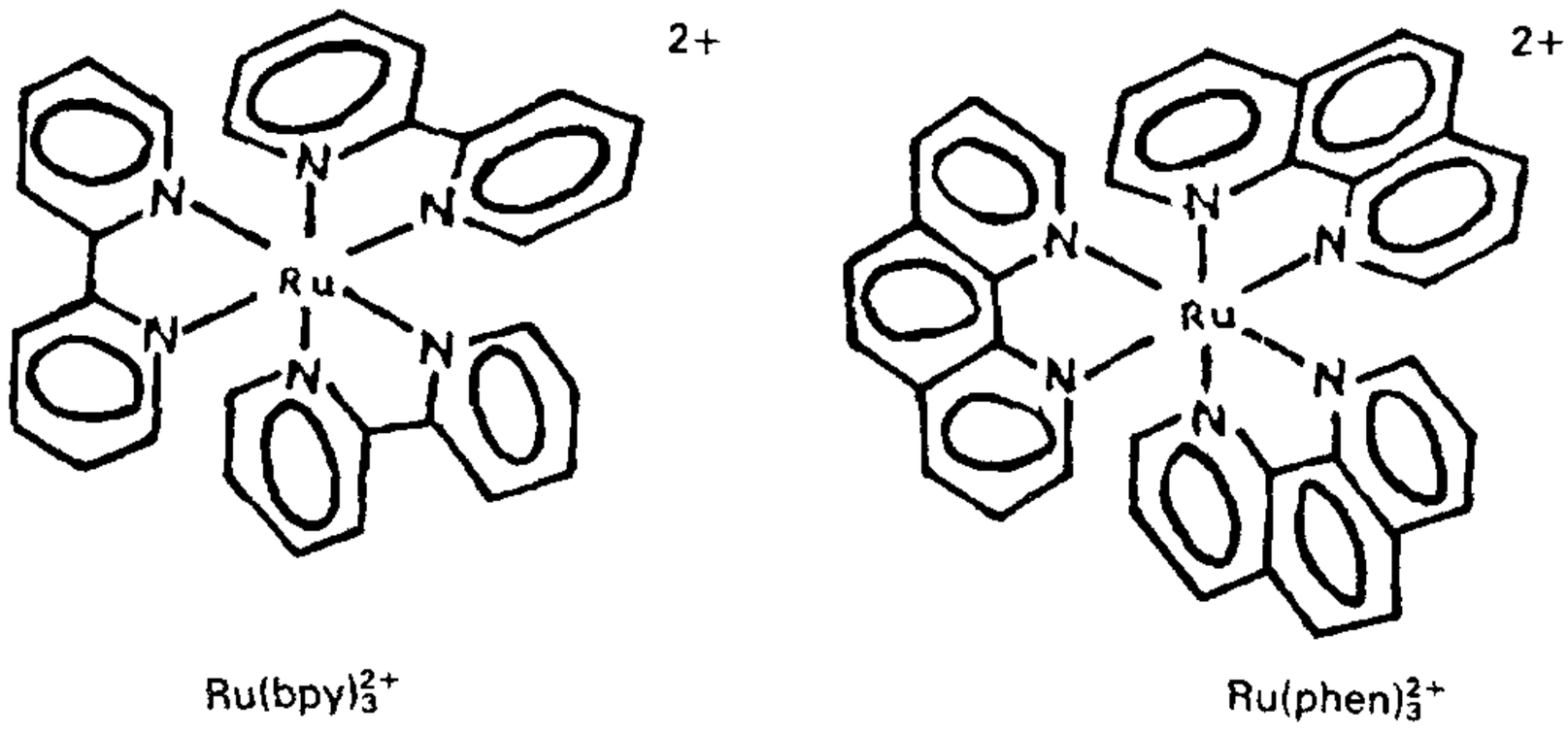

$Ru(bpy)_3^{2+}$ $Ru(phen)_3^{2+}$

Figure 2. Structures of $Ru(bpy)_3^{2+}$ and $Ru(phen)_3^{2+}$.

racemic complex within the clay matrix while Yamagishi had noted discernible differences in packing geometries of enantiomeric and racemic forms of similar complexes[7,8]. Most remarkably, Yamagishi had suggested that these ions intercalate in the clay interlayer as racemic pairs. These observations suggested that racemic pairing may be the driving force for aggregation of the complex within the clay matrix[19], and that such aggregation in turn may lead to non-covalent molecule-molecule interactions which may, at least in part, be responsible for the absorption spectral shifts noted above. Consequently, we examined the spectral profiles of the enantiomeric forms of $Ru(phen)_3^{2+}$ and $Ru(bpy)_3^{2+}$ as well, and the spectra of the latter are shown in figure 3 (traces a and b). As is evident from the figure, these spectra differ from the spectrum of the racemate (trace c), e.g. λ_{max}(MLCT) = 461 nm for absorbed enantiomers vs. 469 nm for absorbed racemate[10]. We emphasize that such spectral differences are not observed when the complexes are dissolved in water or

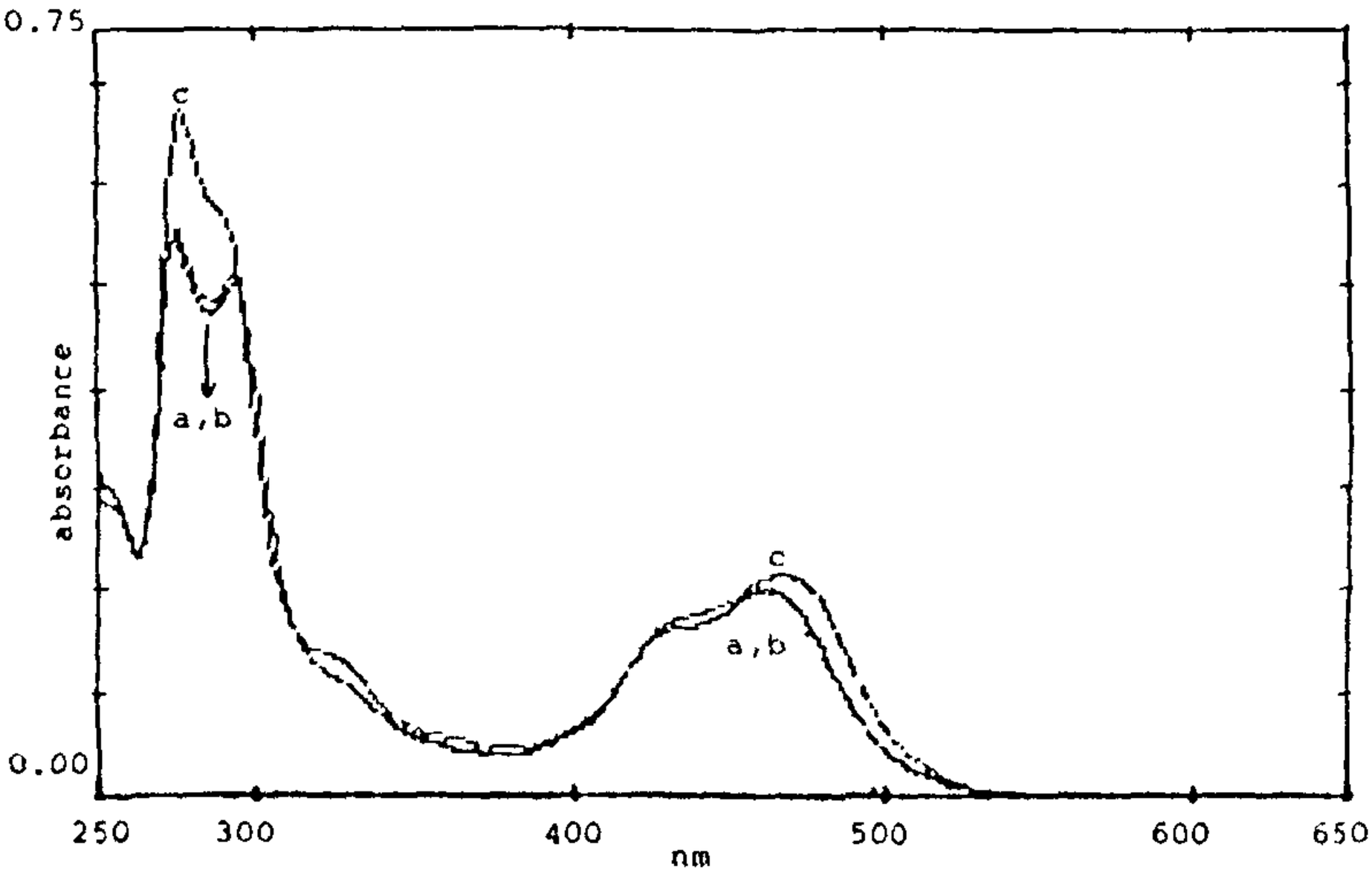

Figure 3. UV-vis absorption spectra of 1.25×10^{-5} M (a) (−)-, (b) (+)-, and (c) (±)-$Ru(bpy)_3^{2+}$ in 1 g/L Na-hectorite. The racemate was prepared by pre-mixing the pure enantiomers prior to adsorption on clay.

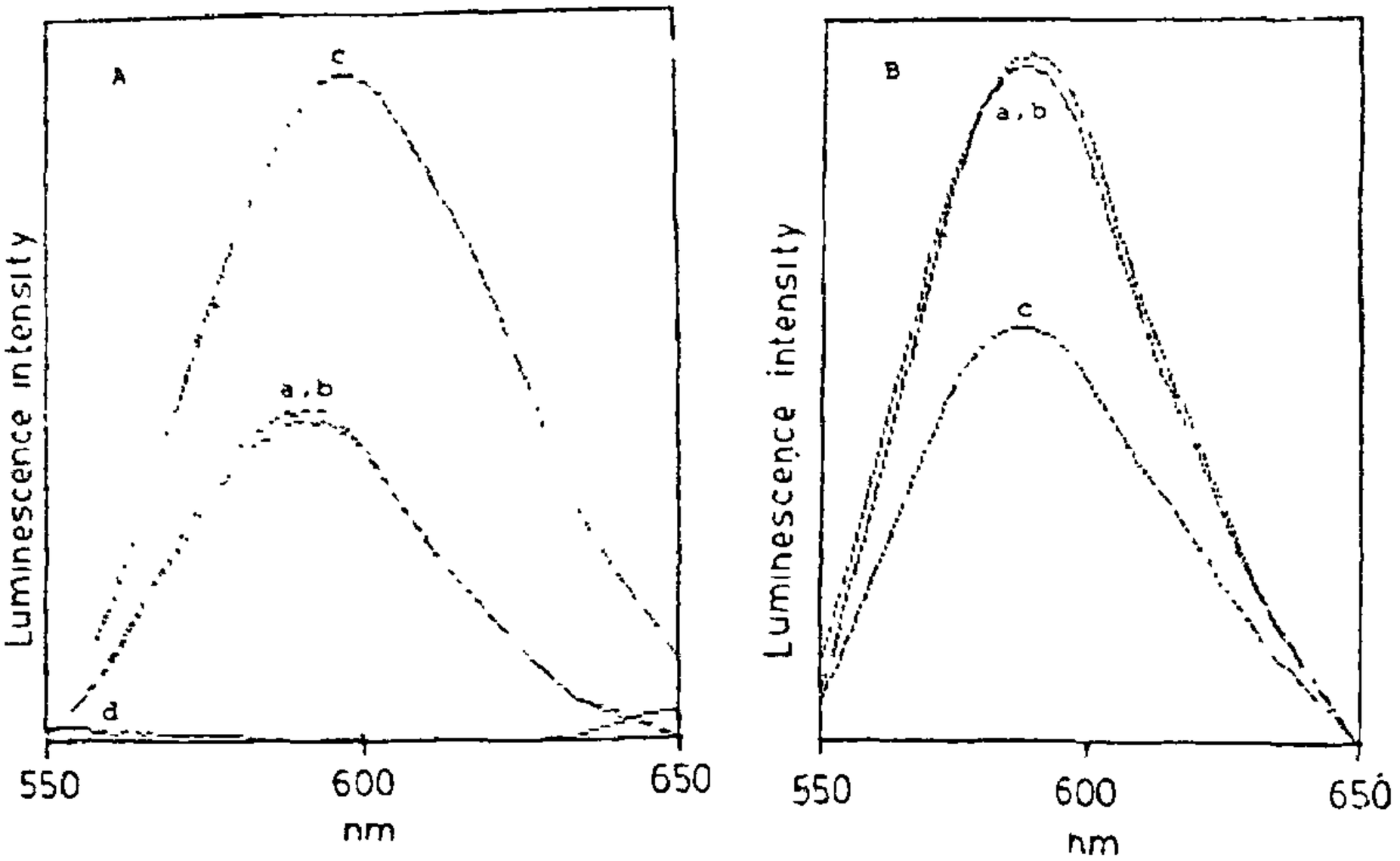

Figure 4. Luminescence spectra (460 nm excitation) of 1×10^{-5} M $Ru(bpy)_3^{2+}$ (A) and $Ru(phen)_3^{2+}$ (B) in 1 g/L Na-hectorite clay; (a) = (−) enantiomer, (b) = (+) enantiomer, (c) = racemate formed by premixing above enantiomers prior to adsorption, (d) = clay sample not containing Ru(II).

adsorbed on SDS micelles or ion-exchange polymers such as Nafion. Thus, smectite clays seem to offer a unique geometry for alignment of the complexes in a manner suitable for interaction between optical antipodes.

Although the uv-vis absorption spectral data have enabled us to distinguish between binding states of the enantiomeric and racemic forms of Ru(II) complexes, the spectral differences are indeed small[9] in the case of $Ru(phen)_3^{2+}$. We therefore proceeded to search for more sensitive probes of binding state differences[10]. Figure 4A shows the luminescence spectra of (+)-, (−)-, and (±)-$Ru(bpy)_3^{2+*}$ in 1 g/L Na-hectorite while figure 4B shows the corresponding spectra of the $Ru(phen)_3^{2+*}$ complex. We have found that the peak emission intensity of racemic $Ru(bpy)_3^{2+*}$ is 60–100% higher than that of the excited enantiomers, and its location is red-shifted by 5–6 nm w.r.t. the enantiomers' spectrum (λ_{max}(emiss)(±) = 596 nm vs. 590 nm for (+)- or (−)-$Ru(bpy)_3^{2+*}$). Surprisingly, the luminescence intensity trend is the opposite in the case of $Ru(phen)_3^{2+*}$, the racemate intensity being 50–60% lower than that of the enantiomers. Further, unlike in the case of $Ru(bpy)_3^{2+}$, the position of the emission maximum is nearly the same for the enantiomers and racemate. Our luminescence spectra therefore show up differences between $Ru(bpy)_3^{2+}$ and $Ru(phen)_3^{2+}$ intercalation not apparent from the uv-vis absorption data. Additionally, the differences between racemate and enantiomers is amplified as a result of the sharp differences in emission intensity of the two forms. Although not pertinent to the present work, we would like to mention recent studies on the luminescence enhancement of MV^{2+} upon adsorption in clay[20].

We have obtained further confirmation of the steady state luminescence spectral difference from time-resolved luminescence studies. These studies indicate a faster decay of (±)-$Ru(phen)_3^{2+*}$-hectorite emission as compared to that of the enantiomeric adsorbates, while the reverse is found with $Ru(bpy)_3^{2+*}$. As in the absorption spectral studies, no differences have been observed in the room temperature luminescence spectra and luminescence decay profiles of the enantiomeric and racemic forms, when these complexes are dissolved in water.

We have also carried out luminescence quenching studies on the Ru(II)-adsorbates. Figure 5 shows. Stern-Volmer plots for the

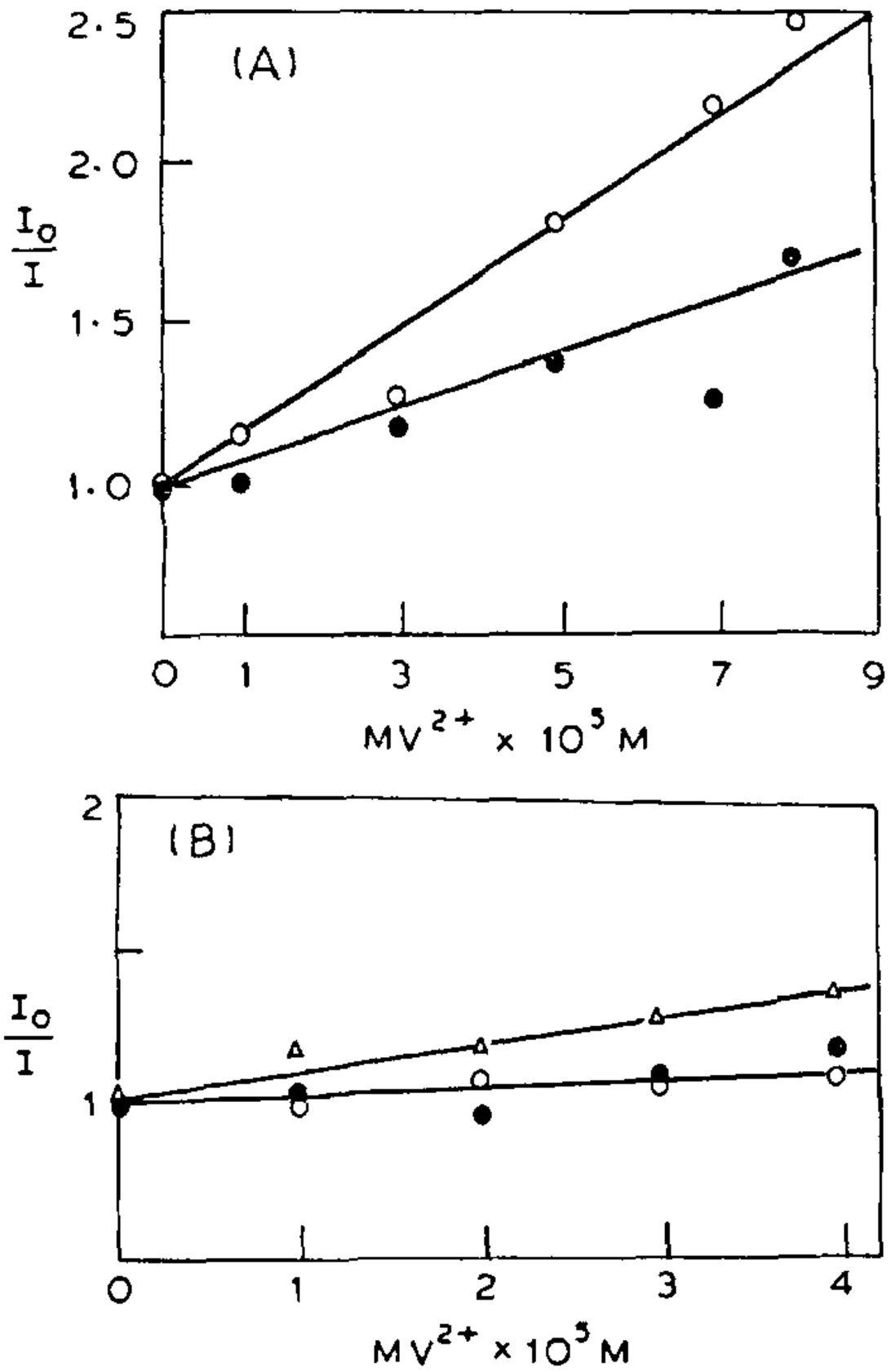

Figure 5. Stern-Volmer plots for the quenching of enantiomeric [● = (+); ○ = (−)] and racemic (△) $Ru(phen)_3^{2+}$ (A) and $Ru(bpy)_3^{2+}$ (B) by methyl viologen (MV^{2+}) in a 1 g/L aqueous Na-hectorite dispersion. MV^2 and the Ru(II) complex were pre-mixed prior to adsorption onto clay. The $Ru(phen)_3^{2+}$ and $Ru(bpy)_3^{2+}$ concentrations were 1×10^{-5} M and 6.5×10^{-6} M, respectively.

quenching of $Ru(phen)_3^{2+*}$-hectorite and $Ru(bpy)_3^{2+}$-hectorite by methyl viologen (MV^{2+}). In these experiments, the Ru(II) complex was pre-mixed with MV^{2+} prior to addition into aqueous Na-hectorite. Analysis of the supernatant following high speed centrifugation confirmed the total sorption of both species in clay so that the effective quencher concentration was ca. three orders of magnitude higher than that shown in the figure. Our results indicate that enantiomeric $Ru(phen)_3^{2+*}$-hectorite is quenched most effectively by MV^{2+} while the quenching is least effective for the enantiomers of $Ru(bpy)_3^{2+}$. Clearly, the quenching trends regarding enantiomers vs. racemate are not the same for the phen and bpy complexes. Assuming bimolecular quenching kinetics, the quenching rate constant (k_q) is estimated to be $3 \times 10^7\ M^{-1}s^{-1}$ for (−)-$Ru(phen)_3^{2+*}$-hectorite and $< 2 \times 10^6\ M^{-1}s^{-1}$ for (−)- and (+)-$Ru(bpy)_3^{2+*}$-hectorite. These values are much smaller than the quenching rate constant in water ($k_q = 1.03 \times 10^9\ M^{-1}s^{-1}$). We believe that the assumption of bimolecular kinetics for quenching within clay may be invalid and that the effective concentration of MV^{2+} "seen" by the Ru(II) complexes is less than the calculated value due to the segregation of these ions in different interlayers. Indeed, we hypothesise that enantiomeric $Ru(phen)_3^{2+*}$ is quenched more effectively than the others since this ion presumably has a binding state that permits maximum accessibility to the MV^{2+} quencher.

We have also studied the quenching of (−)-, (+)-, and (±)-$Ru(phen)_3^{2+*}$-hectorite by (−)-$Co(edta)^-$ (figure 6). Unlike in the case of MV^{2+}, the optically active Co(III) quencher is anionic and therefore interacts only weakly with the clay matrix. It may therefore be assumed that the effective concentration of Co(III) in the clay coincides with the concentration scale shown in figure 6. The surprising aspect about the data in the figure is the lack of

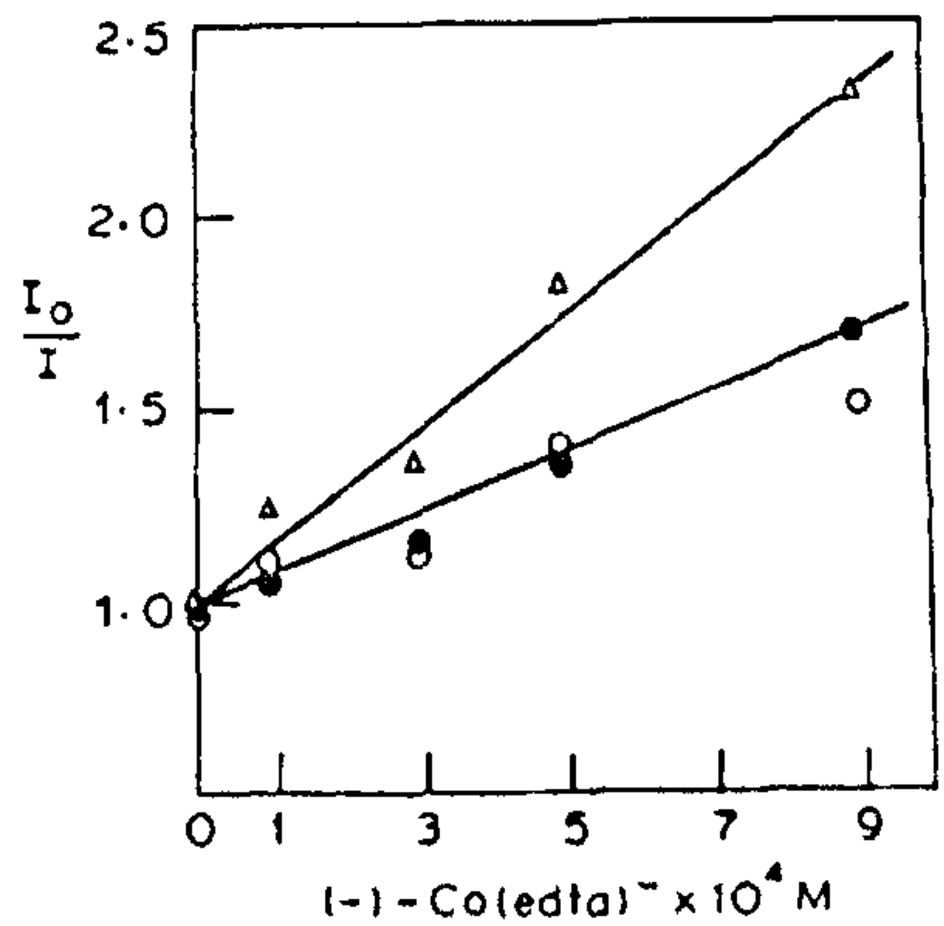

Figure 6. Stern-Volmer Plots for the quenching of 1.5×10^{-5} M (−)-(○), (+)-(●), and (±)-$Ru(phen)_3^{2+}$ (△) by (−)-$Co(edta)^-$ in 0.5 g/L Na-hectorite. The Ru(II) and Co(III) solutions were pre-mixed prior to addition of clay.

discrimination between the (−)- and (+)-enantiomers of $Ru(phen)_3^{2+}$ and the greater efficiency in the quenching of the racemate (calculated $k_q = 2.8 \times 10^9 M^{-1}s^{-1}$ for racemate vs. $1.2 \times 10^9 M^{-1}s^{-1}$ for the enantiomers). These values are somewhat higher[21] than the rate constant in water ($k_q = 0.3 \times 10^9 M^{-1}s^{-1}$), indicating that the concentration of $Co(edta)^-$ may be higher in the clay interlayer than in the bulk solution. A comparison of the quenching data obtained with MV^{2+} and (−)- $Co(edta)^-$, respectively, indicates that the latter is a far more effective quencher of adsorbed $Ru(phen)_3^{2+*}$ than the former, although their quenching efficiencies follow a reverse order in water. We ascribe this to the possible differences in diffusion coefficients between cations and anions and segregation of MV^{2+} from the Ru(II) complex[11]. We note that very facile quenching has been observed with ions which are likely to integrate with Ru(II) in the clay interlayer, e.g. $Co(phen)_3^{3+}$ and $Ni(phen)_3^{2+}$. Results of these studies will be reported elsewhere[22].

CONCLUSION

Steady state and dynamic luminescence spectral studies, with and without the addition of quenchers, have enabled us to comment on the binding state differences between the enantiomeric and racemic forms of poly-(pyridyl)-Ru(II) complexes and to shed light on the differences in sorption modes of seemingly analogous complexes such as $Ru(phen)_3^{2+}$ and $Ru(bpy)_3^{2+}$. However, whether these differences stem from kinetic factors or are due to spontaneous interaction between adsorbed antipodes is unclear at present.

ACKNOWLEDGEMENT

We thank Dr T. Mukherjee and colleagues at the Bhabha Atomic Research Centre, Bombay for providing us with the time-resolved luminescence data and Dr K. Srinivasan for helpful discussions. This work was supported by IEL Limited.

15 February 1988

1. Tsvetkov, F. and Mingelgrin, V., *Clays Clay Miner.*, 1987, **35**, 391, and references therein.
2. (a) Cairns-Smith, A. G., *Sci. Am.*, 1985, **252**, 74; (b) Bernal, J. D., *The origin of life*, Weidenfeld & Nicholson, London, 1967, p. 57; (c) Ponnamperuma, C., Shimoyamaad, A. and Friebele, E., *Origins of life*, 1982, Vol. 12, p. 9. (d) Weiss, A., *Angew Chem. Int. Ed.*, 1981, **20**, 850.
3. Yamagishi, A., *J. Am. Chem. Soc.*, 1985, **107**, 732, and references therein.
4. Kotkar, D. and Ghosh, P. K., *Inorg. Chem.*, 1987, **26**, 208.
5. Yamagishi, A., *J. Electroanal. Chem.*, 1985, **191**, 449.
6. Turro, N. J., Kumar, C. V., Grauer, Z. and Barton, J. K., *Langmuir*, 1987, **3**, 1056, and references therein.
7. Yamagishi, A. and Sóma, M., *J. Am. Chem. Soc.*, 1981, **103**, 4640.
8. Yamagishi, A., *J. Phys. Chem.*, 1982, **86**, 2472.
9. Joshi, V., Kotkar, D. and Gosh, P. K., *J Am. Chem. Soc.*, 1986, **108**, 4650.
10. Joshi, V. and Ghosh, P. K., *J. Chem. Soc., Chem. Commun.*, 1987, 789.
11. Ghosh, P. K. and Bard, A. J., *J. Phys. Chem.*, 1984, **88**, 5519.
12. Braddock, J. N. and Meyer, T. J., *J. Am. Chem. Soc.*, 1973, **95**, 3158.
13. Dwyer, F. P., Gyarfas, E. C. and Mellor, D. P., *J. Phys. Chem.*, 1955, **59**, 296.
14. Dwyer, F. P. and Garvan, F. L., *Inorg. Synth.*, 1955, **6**, 192.
15. Dwyer, F. P. and Gyarfas, E. C., *J. Proc. R. Soc., N. S. W.*, 1949, **83**, 170; *ibid*, 1949, **83**, 174.
16. Van Olphen, H., *An introduction to clay colloid chemistry*, Wiley, New York, 1977.
17. (a) Della Guardia, R. A. and Thomas, J. K., *J. Phys. Chem.*, 1983, **87**, 990; (b) Traynor, M. F., Mortland, M. M. and Pinnavaia, T. J., *Clays. Clay Miner.*, 1978, **26**, 318.
18. Krenske, D., Abdo, S., Van Damme, H., Cruz, M. and Fripiat, J. J., *J. Phys. Chem.*, 1980, **84**, 2447.
19. It is pertinent, in this context, to point out a recent theoretical study (Salem, L., *J. Am. Chem. Soc.*, 1987, **109**, 2887), on the interaction between optical antipodes of tetrahedral organic molecules.

20. Villemure, G., Dettelier, C. and Szabo, A. G., *J. Am. Chem. Soc.*, 1986, **108,** 4658.
21. Kalyanasundaram, K., *Coord. Chem. Rev.*, 1982, **46,** 159.
22. Joshi, V. and Ghosh, P. K. (manuscript in preparation).

ANNOUNCEMENT

IAEA PROGRAMME OF SCIENTIFIC MEETINGS FOR 1988

The Scientific Conferences and Symposia convened by the International Atomic Energy Agency (IAEA) in 1988, are as under:

Conferences:

1. International symposium on applications of dynamic functional studies in nuclear medicine in developing countries, jointly with the World Health Organization (WHO)—Vienna, Austria, 15–19 August; 2. 12th international conference on plasma physics and controlled nuclear fusion research—Nice, France, 12–19 October; 3. International symposium on regulatory practices and safety standards for nuclear power plants, jointly with OECD/NEA—Munich, Germanay F.R., 7–10 November.

International conference on the acceptance, control of, and trade in irradiated food, jointly with the Food and Agriculture Organization (FAO), WHO, the International Trade Centre (ITC)—Geneva, Switzerland, 12–16 December.

Seminars:

1. Regional seminar for European INIS (International Nuclear Information System) experts—Karlsruhe, Germany F.R., 6–10 June; 2. Seminar on the improvement of crops in Africa through the use ot induced mutation, jointly with FAO—Lusaka, Zambia, 20–24 June; 3. Seminar on new approaches in practices and process technology for the radiation sterilization of medical supplies—Laval, Canada, 25–29 July; 4. Seminar on training on nuclear medicine in developing countries, jointly with WHO—Vienna, Austria, 8–12 August; 5. Seminar on radiation protection services for developing countries in Africa—Nairobi, Kenya, 5–9 September; 6. Seminar on industrial radiation applications for the region of Latin America—Quito, Ecuador, 3–6 October; 7. INIS training seminar for Asia and the Pacific for input preparation and output utilization—Beijing, China, 10–15 October, and 8. Seminar for Asia and the Pacific on nuclear techniques in parasitic and communicable diseases—Bombay, India, 21–25 November.

Detailed information may be obtained from the appropriate national authorities in Member States, such as the Ministry of Foreign Affairs and the National Atomic Energy Commission or by writing directly to the International Atomic Energy Agency, P.O. Box 100, Vienna International Centre, A-1400 Vienna, Austria.